Kinetically Controlled Aggregation in Reactive Adsorbate Overlayers

OREN M. BECKER,[a] MARVIN SILVERBERG[b]* AND AVINOAM BEN-SHAUL[a]**
[a]Department of Physical Chemistry and The Fritz Haber Research Center for Molecular Dynamics, The Hebrew University of Jerusalem, Jerusalem 91904, Israel
[b]Department of Chemical and Biological Sciences, Oregon Graduate Center, 19600 N.W. Von Neumann Drive, Beaverton, OR 97006-199, USA

(*Received 7 June 1989*)

Abstract. The kinetics of surface chemical reactions depend critically on the lateral distribution of the adsorbed reactants. In some cases, the adsorbates are aggregated into islands and the rate of reaction is strongly influenced by the structural (sizes and shapes) and energetic (lateral interaction potentials) characteristics of the aggregated overlayer. Adsorbate aggregation or segregation on surfaces may be induced by a variety of mechanisms, three important types of which are briefly discussed here. The first process is driven by strong lateral interactions between the adsorbed particles, which favor their organization in an ordered two-dimensional phase, but because of kinetic constraints the system only reaches a long-lived metastable state characterized by finite islands with highly ramified edges. A somewhat more complex aggregation–segregation process, in a system comprised of two interacting adsorbate species, is also described, and the consequences with respect to surface reaction kinetics are demonstrated. The second aggregation process reflects (Eden-type) island formation during adsorption of molecules from the gas phase. More specifically, these islands result from the so-called (extrinsic) precursor-mediated chemisorption mechanism. Finally, we discuss the segregation of adsorbed reactants induced by the bimolecular annihilation reaction $A + B \rightarrow 0$, under steady-state conditions. Unlike in the first example, this segregation process takes place even in the absence of adsorbate interactions (except for the reactive A–B interaction) and is most pronounced in the absence of particle diffusion.

1. INTRODUCTION

Aggregation and segregation phenomena in molecular systems are driven by different types of interactions between the constituent particles. Common examples are molecular (van der Waals) clusters in the gas phase, in solution, or on surfaces, which are held together by long-range attractive intermolecular forces. At low enough temperatures (below critical), these forces induce the formation of macroscopic aggregates, namely, condensed phases. In general, segregation processes take place in systems containing two (or more) species in which the attractive interactions between like particles are stronger than the (average) attraction between unlike particles.[1-7] An example of relevance to the forthcoming discussion is that of a mixed adlayer of A and B molecules on a solid surface. If only nearest-neighbor lateral interactions between the adsorbates (w_{AA}, w_{AB}, w_{BB}) are important, local segregation into A-rich and B-rich regions will take place if $w_{AB} - (w_{AA} + w_{BB})/2 > 0$.[1-3] Below a critical temperature T_c, the system tends to undergo macroscopic phase separation.

Quite often in real systems the thermodynamic tendency favoring aggregation, segregation, or phase separation is only partially accomplished, because of kinetic constraints.[8] An example which will be discussed in some detail in the next section is that of an adlayer of atoms or molecules (e.g., oxygen atoms or

* Present address: Department of Chemistry, Northwestern University, Evanston, IL 60208, USA.
** Author to whom correspondence should be addressed.

carbon monoxide molecules on platinum) interacting via nearest-neighbor (NN), or higher order, attractive forces.[9,10] Suppose that the adsorbates are initially distributed randomly on the surface, as would be the case following (nonselective) adsorption from the gas phase, or quenching from a high temperature. If $T < T_c$, where T_c is the critical temperature of the two-dimensional (2D) gas–solid transition, the adatoms tend to reorganize into large domains of a 2D solid, coexisting with a dilute 2D gas. This condensation process is brought about by particle diffusion on the surface ending up with "sticky collisions." As we shall see in the next section, following a relatively fast stage at the end of which most atoms are associated in finite aggregates, the system is kinetically "stuck" in this long-lived metastable state.[2,3] The main reason for the incomplete phase separation is that, unlike in the gas phase or in solution, where cluster–cluster coalescence is a fast and crucial pathway to the formation of macroscopic aggregates, in the case of adsorbate clusters this is a very inefficient process. Of course, the size distribution of the adsorbate islands in the long-lived intermediate state and their highly nontrivial patterns involve important consequences with respect to surface reaction kinetics, as will be briefly discussed in Section 2.

The case of "frustrated thermodynamic tendency" described above is just one of many examples in which kinetic factors play a central role in aggregation processes and in affecting the structural characteristics of the resulting aggregates. In fact, the classification and characterization of kinetically controlled aggregation phenomena has become a very active research field in recent years.[11,12] To a large extent this is due to the growing interest in fractal aggregates such as percolation[13] or Witten–Sanders (DLA = diffusion limited aggregation) clusters.[14] Some kinetically controlled growth mechanisms, such as DLA, yield highly ramified clusters, while others result in the formation of more compact aggregates, e.g., those known as Eden-type clusters.[11]

In Section 3 we describe a model for the chemisorption of atoms on solid surfaces, incorporating both "direct" chemisorption onto vacant sites and "indirect" (or "precursor-mediated") chemisorption initiated by physisorption on top of occupied sites. We shall see that the second pathway implies an island growth mechanism generating Eden-type 2D clusters. As in the previous example, if the chemisorbed molecules are about to participate as reactants in a surface reaction, the geometric characteristics of the islanded overlayer can play a crucial role in the kinetics of this reaction.

A third example of an aggregation–segregation process of adsorbates on surfaces, which is of direct relevance to surface reaction kinetics, will be discussed in Section 4. We shall describe there the steady-state behavior in a bimolecular surface reaction, $A + B \rightarrow 0$, in which 0 designates a rapidly desorbing AB product. More specifically, in this system constant fluxes of A and B molecules impinge on the surface, and reaction takes place if the adsorbed A and B molecules happen to occupy adjacent adsorption sites. Obviously, since A and B annihilate each other whenever they become neighbors, the reaction induces segregation of A's and B's into separate regions.[15] On the other hand, the structure of these regions, as well as that of the vacant sites, which dictate the steady-state reaction rate, is not so obvious. In Section 4 we shall consider some of the pertinent questions in little more detail.

Due to the complexity of the aggregation and segregation processes of the type mentioned above, their theoretical description in terms of closed-form (analytical) mathematical expressions is often not feasible. Consequently, computer simulations, mostly of the Monte Carlo (MC) variety, have emerged as a major tool in the study of aggregation phenomena and pattern formation.[16] (In fact, some of the more interesting structures have first been reported as computer experiments.) Similarly, in the following sections, we shall use snapshots from MC simulations to visualize the appropriate aggregation patterns and overlayer structures. It should be noted, however, that in some cases approximate analytical approaches, complementing or replacing the MC simulation, are possible and useful. For example, in a system governed by simultaneous kinetic processes involving very different time scales, one can apply analytical approximations for the fast ones, retaining the MC algorithm for the slow ones only. The implications of this notion to the kinetics of an $A + B \rightarrow 0$ reaction, in which A is aggregated and immobile whereas B diffusion is rapid, will be briefly considered in Section 2. In general, the discussion below will be rather qualitative, emphasizing the physical aspects and avoiding the mathematical details.

2. AGGREGATION INDUCED BY ADSORBATE INTERACTIONS

Consider a bimolecular surface reaction

$$A(s) + B(s) \rightarrow 0 \qquad (0 = AB(g)) \qquad (1)$$

in which A(s) and B(s) are the adsorbed reactants (s = surface; g = gas), and the symbol 0 means instantaneous desorption of the AB(g) product.[2–4] In other words, as far as surface coverage is concerned, Eq. (1) is a pair annihilation reaction. Reactions of this type are

common in surface catalysis, the $O + CO \rightarrow CO_2$ reaction on Pt and other metals being one of the standard examples.[10]

Except for limiting cases, such as when A and B are randomly distributed on the surface, the rate, R, of reaction (1) is not a simple function of the coverages θ_A and θ_B. In general, the rate can be expressed as:

$$R = -\frac{d\theta_A}{dt} = \frac{1}{M}\sum_{(n,m),s} P(A_n, B_m; s)q(s). \qquad (2)$$

Here $P(A_n, B_m; s)$ is the joint probability that two neighboring adsorption sites n and m will be occupied by A and B atoms, respectively, and that this potentially reactive A–B pair will be surrounded by A and B neighbors (and vacancies) as specified by the local surroundings s. $q(s)$ is the reaction probability per unit time of this pair. The (n, m) summation is over all relevant pairs of adsorption sites; e.g., if only NN A–B pairs are reactive, there are $M \cdot z$ such pairs. M is the total number of lattice adsorption sites and z is the lattice coordination number. Similarly, the s summation is over all neighbor configurations within the range of interaction with the central, reactive, pair.

$P(A_n, B_m; s)$ reflects the lateral distribution of the adsorbed reactants on the surface, and we thus refer to it as the "topological" (or "geometrical") factor in the reaction rate. This probability is strongly dependent on initial conditions, such as the order and time lag between the adsorption of the two reactants, the surface temperature, and the initial coverages. It also depends on adsorbate–adsorbate interaction potentials as well as on the rates of A and B diffusion and of the A + B reaction. In the very special case that A and B are randomly distributed, the probability of finding any site, n, populated by A is θ_A, and the probability of finding any of its z neighbors occupied by B is θ_B. Hence $P(A_n, B_m; s) = z\theta_A\theta_B P(s)$ with $P(s)$ denoting the probability of a local surrounding s (which can be similarly calculated). If $q(s) = q$ is independent of s, we obtain $R = z\theta_A\theta_B q$.

Two conditions must be satisfied in order that the 2D distribution of A, B will be random.[2] Firstly, A and B diffusion should be faster than any other kinetic process in the system, reaction in particular. Secondly, adsorbate–adsorbate interactions must be negligible, i.e., $w_{ij}/kT \ll 1$. These conditions are rarely met in realistic systems. For instance, in the $O + CO \rightarrow CO_2$ reaction on Pt or Pd surfaces, the oxygen atoms are essentially stationary in the course of the reaction. Furthermore, the interaction potentials between the adsorbates are typically $|w| \sim 0.1$ eV, i.e., $w/kT \sim 1$ at the common temperature range of surface reactions, $T \sim 300$–600 K.[8–10,17]

Lateral interaction energies can strongly affect the activation barriers to diffusion and reaction.[3,4] To a first approximation, the effect of these interactions on the reaction probability, q in Eq. (2), can be accounted for using a modified Arrhenius form,

$$q(s) = \nu \exp[-(\varepsilon_0 - w_s)/kT] = q_0 \exp(w_s/kT), \quad (3)$$

where $q_0 = \nu \exp(-\varepsilon_0/kT)$ is the reaction probability of an isolated A–B pair, ν denoting the frequency factor and ε_0 the bare activation energy. The lateral interactions of the potentially reactive A–B with their neighbors appear in w_s. If for instance only nearest-neighbor interactions are important, then we expect $w_s = n_{AA}w_{AA} + n_{BB}w_{BB} + n_{AB}w_{AB}$, where out of the $2z-2$ "bonds" connecting the reactive pair to its NN surrounding n_{AA} is the number of A–A bonds, etc. In general, if $w_s < 0$, i.e., the reactive pair is (on the average) attracted by its neighbors, the effective activation barrier $\varepsilon_0 - w_s$ will be higher than that of the bare pair and, correspondingly, $q(s)$ will be smaller. On the other hand, repelling neighbors ($w_s > 0$) enhance the reaction probability. Note that since the w_{ij}'s are of order kT the effect on $q(s)$ can be most significant, e.g., if $w_{AA} = -2.5kT$, every A–A bond will reduce q by a factor $x = \exp(w_{AA}/kT) \sim 0.1$. Thus for example in the $O + CO \rightarrow CO_2$ system, where the oxygen atoms tend to aggregate, it is expected that isolated oxygen atoms will be more reactive than those associated in pairs, the latter will be more reactive than those atoms with two neighbors around, etc. Consequently, the coastlines of oxygen islands will become gradually smoother as reaction proceeds. All these effects of lateral interactions on the reaction probability enter via the "energetic factor"[3,4] $q(s)$ in Eq. (2).

The qualitative notions discussed above have been analyzed in considerable detail for a variety of model[2,3] as well as realistic systems.[4] Various schemes of initial conditions, lateral interaction potentials, diffusion and reaction rates have been studied using MC simulations, approximate lattice gas models (such as the Bragg–Williams and the Guggenheim quasi-chemical or Bethe–Peierls schemes) and combinations thereof.[2–4] In the general spirit of this article, we have chosen to very briefly illustrate here some of the structural and temporal characteristics of adsorbate islanding in two systems of the $A + B \rightarrow 0$ family. A simple one, in which we focus on the effects of NN A–A attractions, and a more complex system illustrating the role of longer range A–A, B–B, and A–B interactions.

Figure 1 illustrates several stages in the aggregation

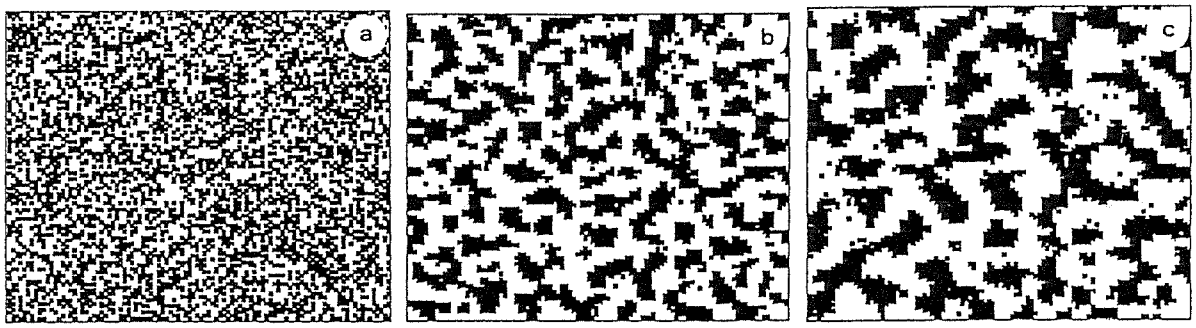

Fig. 1. Three stages in the island formation of A atoms with attractive NN interactions $w_{AA}/kT = -2.5$ and coverage = 0.4: $t = 0$ (a); $t = 1000$ MCS (b); $t = 5000$ MCS (c). Shown are 100×100 sections of the 500×500 lattice used in the calculations. (MCS = 1 Monte Carlo step[2]).

process of particles with NN A–A attractions.[2,3] The particles are initially adsorbed randomly onto the available sites up to a coverage of 0.4 and then undergo activated diffusion. After a short time has passed, most of the particles have been incorporated into small islands. As time evolves, these small islands slowly reorganize through single atom diffusion into larger ones (i.e., via an evaporation–condensation process, no cluster diffusion is allowed). After large islands have formed, the rate of change of their distribution slows down. Note the highly ramified (though "nonfractal") edges of the islands. The implications of these island patterns with respect to reaction kinetics (upon addition of a second, reactive, adsorbate) have been considered above.

Figure 2 shows several stages of a more complex system in which longer range A–A, B–B, and A–B interactions are present.[4] First, the A atoms are adsorbed and diffusion commences. Infinite nearest neighbor repulsion and moderately strong second nearest-neighbor repulsion, combined with mild third nearest-neighbor attractions, induce the formation of a $p(2 \times 2)$ overlayer. Following A rearrangement, B atoms are adsorbed randomly onto the remaining sites. Very strong B–B and A–B repulsions result in segregation of A and B into separate domains. The internal structure of the A domains has been changed in some regions to the more compact $c(2 \times 2)$ configuration. When the temperature is raised and reaction proceeds, two stages of reaction appear. First, at low temperatures, we find a "contact regime" in which reaction occurs between A and B atoms pinned against each other at the edges of their respective regions. After these atoms react, A and B atoms initially located further

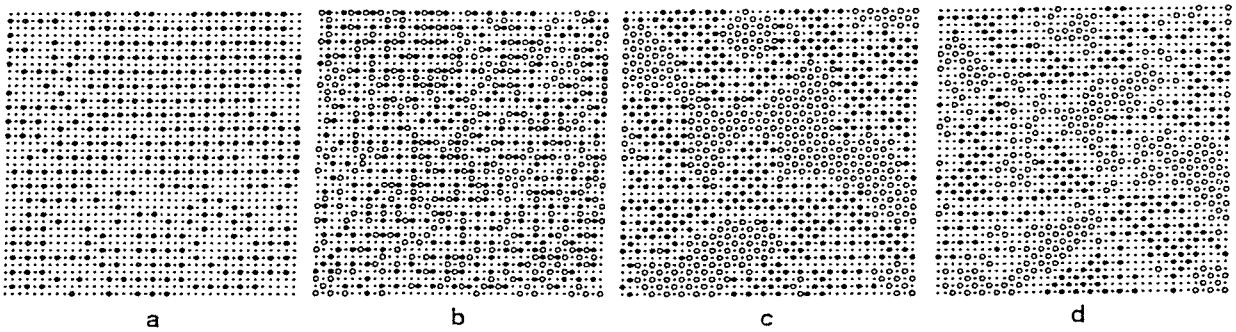

Fig. 2. Several stages of the aggregation and reaction process for the A + B → 0 system. The coverages of the A and B atoms are $\theta_A = \theta_B = 0.2$. Shown are 40×40 sections of the 100×100 lattice used in the calculation. The lateral interaction parameters are $w_{AA,1} = \infty$, $w_{AA,2} = 1.6$ kcal/mol, $w_{AA,3} = -0.6$ kcal/mol. Furthermore, $w_{BB,1} = 4$ kcal/mol, $w_{AB,1} = w_{AB,2} = 3$ kcal/mol. All other $w_{BB,i}$, $w_{AB,i}$, and $w_{AA,i}$ are zero. a. The configuration after A adsorption and 10000 MCS of diffusion. b. Shortly after adsorption of B into available sites. c. Following 10000 MCS of mutual diffusion and segregation. d. The configuration while the reaction is in progress (after a temperature ramp). "The contact regime" has almost ended (boundary atoms have reacted) and further reaction will be diffusion-initiated.

within the separate regions are free to diffuse towards each other and react. This "diffusion regime" of reaction proceeds at higher temperatures, and the reagent islands shrink due to diffusion-induced reaction.

3. ADSORPTION-INDUCED AGGREGATION

In the simplest, classical, adsorption model of Langmuir, the adsorbed molecules are assumed to be randomly distributed among the adsorption sites, and additional gas-phase molecules can only be adsorbed ("directly") onto the remaining vacant sites.[17] Consequently, the adsorption probability at coverage θ is given by $S(\theta) = S_0(1 - \theta)$, with $S_0 = S(\theta \to 0)$ denoting the sticking probability on the bare surface. Extended models have been proposed by several authors to explain deviations from Langmuirian behavior, which in many cases, especially in chemisorption systems, can be very significant.[17,18,20] One well-known model, which has been formulated by Kisliuk[18] thirty years ago and is still in use today, is based on the assumption that in order to become chemisorbed, the gas-phase molecules need not arrive directly on top of vacant sites. Instead, they can be initially trapped (i.e., physisorbed) either above vacant sites ("intrinsic precursor") or above occupied sites ("extrinsic precursor"). The precursor molecules then either desorb back into the gas phase or migrate laterally. Molecules arriving on top of vacant sites may become chemisorbed there. Thus, the intrinsic precursor-mediated chemisorption essentially leads to a Langmuirian behavior. On the other hand, the extrinsic precursor-mediated chemisorption presents an additional, "indirect", possibly most significant pathway to chemisorption.

These notions can be cast in simple mathematical terms leading to a simple expression for $S(\theta)$, namely $S(\theta) = S_0(1 - \theta)/(1 - \alpha\theta)$, where α is proportional to the ratio between the lateral diffusion and desorption rates of an extrinsic precursor molecule. Recall that these molecules are initially trapped above occupied sites and must execute one or more lateral jumps in the second layer before finding an available, vacant, chemisorption site. If chemisorption occurs with unit (or high) probability whenever a physisorbed molecule arrives at a vacant site, it is clear that, once chemisorbed, an extrinsic precursor molecule will occupy a site neighboring another occupied site. In other words, the indirect chemisorption pathway leads to spatial correlations between the chemisorbed molecules.[19] Although the existence of such correlations has been appreciated by Kisliuk,[18] in his model as well as in several other related models[17,20] the lateral distribution of the admolecules is assumed to be random at all times. Clearly, this assumption is valid only if the lateral diffusion rate of the chemisorbed molecules is much faster than the rate of adsorption, an assumption which in many systems is not justified.

Kisliuk's assumption of random adsorbate distribution has been invoked for mathematical simplicity. Today, due to the experience gained in computer simulation studies, it has been realized that the process of precursor-mediated chemisorption closely resembles the growth mechanism leading to the formation of Eden clusters.[19,23] There are several, slightly different, types of Eden clusters, depending on the details of the growth algorithm.[11,12] A common characteristic of all such clusters is their "nonfractal" structure. Namely, these are rather "compact" aggregates characterized by relatively smooth boundaries (except for a certain degree of roughness) and typically of an asymptotically round shape.

Several stages of an island growth process corresponding to the precursor-mediated mechanism are depicted in Fig. 3. Specifically, in this simulation a particle is added at random on top of an already adsorbed particle and executes a random walk in the second layer until it arrives at the island's edge. It can then jump into a neighboring empty site (and chemisorb), thus leading to island growth, or continue to walk, back into the island or along the coastline. (This process, which evidently generates an Eden-type cluster, is very similar to the Eden growth mechanism of type B, according to the classification in Ref. 12). The description above also explains the absence of tortuous defects (such as deep fjords or elongated peninsulas) along the island's coastline. Concave defects (such as fjords) can be approached by random walkers arriving from several directions, while only one direction connects a convex defect to the rest of the island.

In the precursor-mediated chemisorption mechanism described above, we have ignored the possible role of adsorbate–adsorbate interactions. Attractive adsorbate interactions can affect the chemisorption process in two major ways. First, they can significantly enhance the trapping probability of gas-phase molecules on top of an island of adsorbed molecules. In fact, since the physisorbed (extrinsic precursor) molecule is attracted by several molecules located underneath it, the trapping probability can be higher than that on top of vacant sites, thus leading to an increase of $S(\theta)$ with θ (at low coverage). This behavior has been demonstrated using a combined Monte Carlo rate equation approach by Hood et al.[5] and later discussed in general terms in Ref. 19. The second effect of adsorbate–adsorbate attractions is to increase the chemisorption probability at

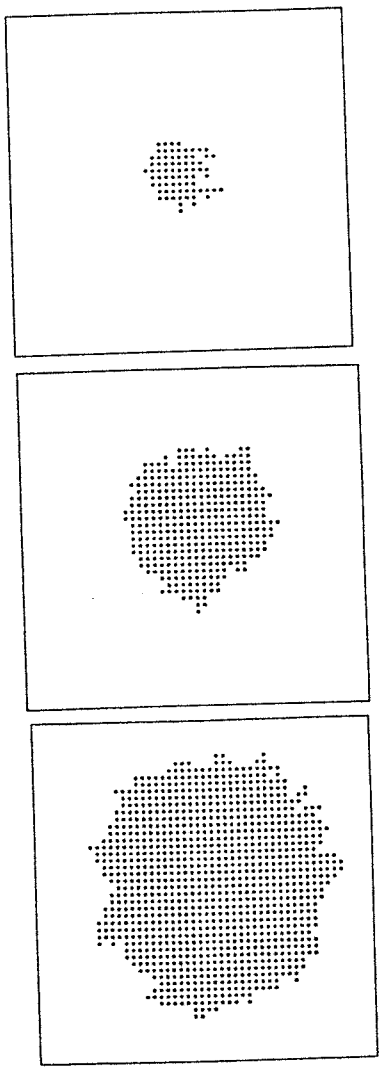

Fig. 3. Three stages in the growth of a single Eden cluster around a preadsorbed seed via the precursor-mediated mechanism.

island edges, particularly at concave regions, where (on the average) a newly arriving molecule will form more attractive "bonds" than it would in a convex region. The result is that the islands will be even smoother than in a simple Eden growth process.

At low coverages one can treat the chemisorption as a sum of two processes: (i) direct adsorption onto vacant sites, as in Langmuir's model. The molecules chemisorbed in this way serve as "seeds" for the second process; (ii) island growth, via the extrinsic precursor pathway described above. Therefore, the rate of change of the coverage (hence also the sticking probability) can be expressed as[19]

$$\dot{\theta} = JS(t) = g(t) + \int_0^t g(u)\dot{K}(t-u)du. \qquad (4)$$

Here J is the flux of molecules impinging on the surface, $g(t)$ is the seeding rate ($g(t) = JS_0[1-\theta(t)]$ in the Langmuirian approximation), and $K(t)$ is the (average) size of an island of "age" t. Equation (4) can be solved, analytically or numerically, depending on the form of $K(t)$, for various cases of interest. The notion that the chemisorbed islands are compact (Eden) aggregates, simplifies the analysis significantly. For instance, in the case of an extrinsic precursor with a short lifetime (i.e., high desorption probability), only those molecules physisorbed in the island's coastline region have a chance to become chemisorbed; hence, $\dot{K} \sim K^{1/2}$ because the perimeter length of a compact island is proportional to the square root of its length. $\theta(t)$ and $\dot{\theta}(t)$ curves for this and other simple cases have been reported elsewhere.[19] Furthermore, based on Eq. (4), one can also calculate more detailed characteristics of the adlayer, such as the island size distribution and its moments.[21]

Equation (4) has a simple interpretation as long as islands grow independently. At coverages on the order of $\theta \sim 0.5$ or higher, island–island coalescence becomes increasingly important and the assumption of independent island growth is no longer justified. This is clearly displayed in Fig. 4 which contrasts the adlayer structures at low and high θ. (Note that since large islands grow faster, most of the atoms at low θ are incorporated in relatively large islands. The simulation of Fig. 4 corresponds to the $\dot{K} \sim K^{1/2}$ growth rate described above.)

The onset of appreciable island overlap around $\theta \sim 0.5$ is not very surprising when we recall that this is (approximately) also the so-called "jamming limit" in the problem of random sequential addition (RSA),[22] as well as the percolation threshold in 2D.[12,13] Recall, however, that we are dealing here with a highly polydisperse distribution of particle sizes, which varies in time and with initial conditions. Thus, a quantitative analysis of the chemisorbed adlayer structure is surely nontrivial. In this context, it is appropriate to mention the MC simulations and the analytical analyses of Sanders and Evans[23] and Anderson and Family.[24] These authors have carefully analyzed the structural characteristics of an overlayer generated via Eden-type growth models. Their analyses include identification of the percolation threshold, fractal dimension, and critical exponents. They conclude that in many respects the scaling behavior of the system resembles that of random percolation. Additional relevant studies on related issues have been published by Evans and co-workers.[6]

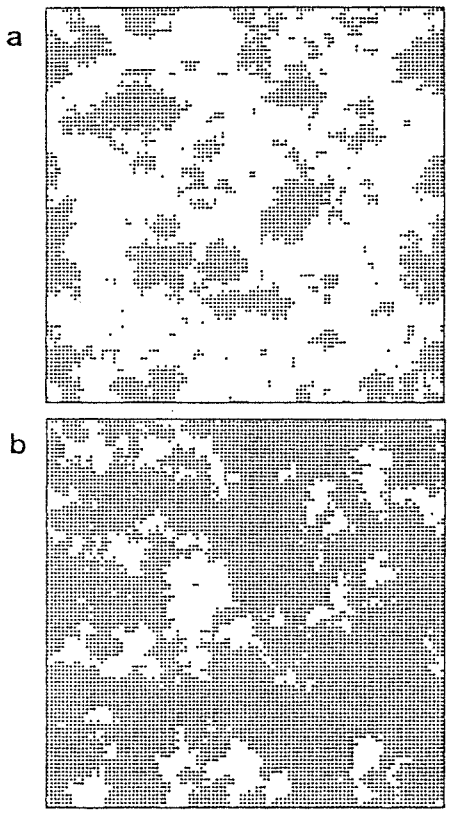

Fig. 4. Adsorption overlayers on a 100×100 surface constructed through the precursor-mediated mechanism; $\theta = 0.3$ (a) and $\theta = 0.8$ (b). The parameters used are: the ratio between physisorption trapping and direct chemisorption, $S_1/S_0 = 1000$, and the rates of the physisorbed molecule diffusion $w_l/J = 10000$ and desorption $w_d/J = 1000$ (J = impingement flux).

4. REACTION-INDUCED SEGREGATION

In Section 2 we have demonstrated the effects of adsorbate lateral interactions in the $A + B \rightarrow 0$ reaction. In particular, we have emphasized the crucial interplay between the lateral interactions and lateral diffusion rates in determining the temporal and structural characteristics of the aggregating adlayer. In this section we return to the annihilation reaction (1) and to demonstrate an entirely different aggregation–segregation mechanism in which lateral interactions are not important and adsorbate diffusion on the surface is totally absent.

Consider a catalytic surface reaction of the type $A + B \rightarrow 0$ in which constant fluxes, J_A and J_B, of A and B molecules from the gas phase strike the surface and the molecules are adsorbed (on vacant sites only) with probabilities S_A^0 and S_B^0, respectively. Thus, the net adsorption rates of A and B are $\phi_A = J_A S_A^0$ and $\phi_B = J_B S_B^0$, respectively. To simplify the model, let us assume that A and B diffusion on the surface can be completely ignored and, in addition, that reaction between A and B occurs with unit probability *whenever* the two reactants occupy nearest-neighbor adsorption sites. (Both assumptions can be relaxed, thereby affecting of course the overlayer structure and kinetics, see below.) That is, if a B molecule happens to arrive at a vacant site which is a neighbor of an A-occupied site, reaction will take place and both A and B will desorb into the gas phase (as an AB molecule), and similarly so if an A molecule arrives at a nearest-neighbor site to a B admolecule. Clearly, this scheme implies segregation of A's and B's to different regions, for the very simple reason that A and B can never be neighbors of each other.

Figure 5 illustrates the overlayer structure predicted by MC simulations corresponding to the above model, starting from different initial conditions. (For simplicity we set $S_A^0 = S_B^0 = 1$ in all simulations.) Note that the simulation has been performed for $\phi_A = \phi_B$ because any other flux ratio would lead to eventual poisoning (i.e., single-component saturation) of the surface. For instance, if $\phi_A > \phi_B$, then after some time the surface will be completely covered by A's because every B arriving at the surface will be consumed by the majority species. Choosing the right flux ratio is thus essential for steady-state operation of the system. It should be noted, however, that the simple $A + B \rightarrow 0$ model is rather singular, as it exhibits a steady state only at one flux ratio, $\phi_A/\phi_B = 1$. In other reaction schemes, such as $A_2(g) \rightarrow 2A(s)$ and $B(g) \rightarrow B(s)$ followed by $A(s) + B(s) \rightarrow 0$ (with s = surface; g = gas), there is a (finite) range of ϕ_A/ϕ_B values for which steady-state reaction is possible.[25,26] Moreover, such schemes resemble more closely the mechanism of realistic catalytic surface reactions, such as the $O_2(g) \rightarrow 2O(s)$, $CO(g) \rightarrow CO(s)$, $O(s) + CO(s) \rightarrow CO_2(g)$ system. It should be noted that the $A_2 \rightarrow 2A$, $A + B \rightarrow 0$ scheme has been rather extensively analyzed both by MC simulations[25,27] and using analytical (lattice gas type) approximations.[26] We have chosen to discuss here the $A + B \rightarrow 0$ scheme for simplicity only.

Although the cause of segregation in the $A + B \rightarrow 0$ scheme is obvious, our understanding of the overlayer structure is still incomplete. Wicke et al.[28] were the first to employ a reaction scheme of this kind, in an attempt to understand the oscillatory reaction rate in the steady-state operation of the $O + CO \rightarrow CO_2$ system. However, these authors have been particularly interested in the high flux limit (where the surface is fully covered by A's and B's and the A + B reaction is not instantaneous)

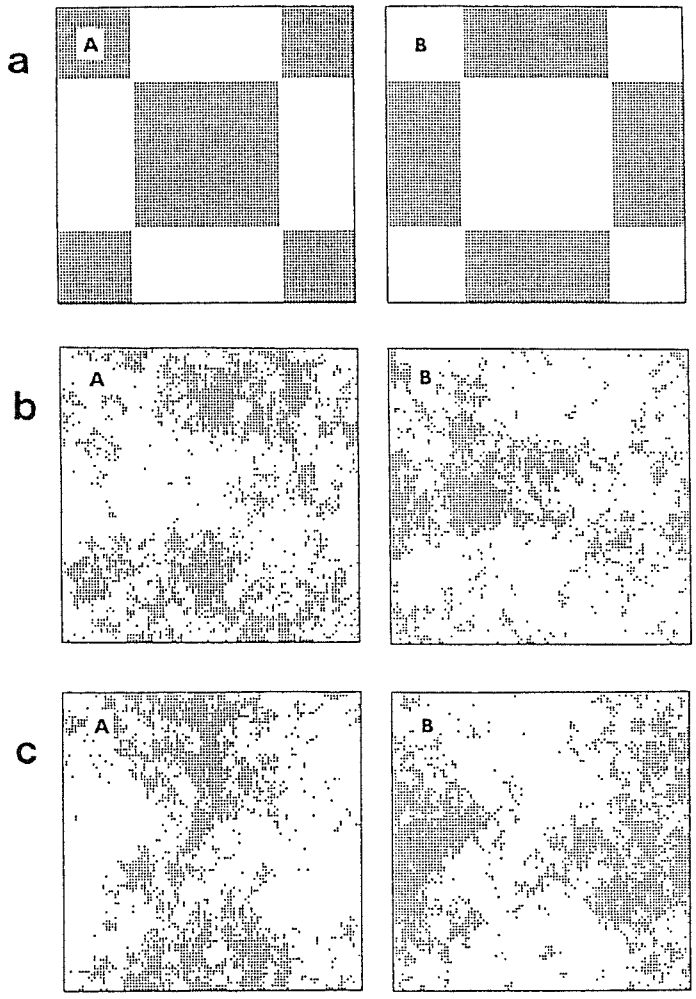

Fig. 5. Distribution of A and B particles on the surface in the annihilation reaction A + B → 0. For clarity, the distributions of A's and B's have been separated and are shown in the left-hand column and in the right-hand column of the figure, respectively. The results shown correspond to constant and equal fluxes of A and B, $J_A = J_B = \text{const}$. The simulations were carried out on a 100×100 square lattice. a. Initial distribution corresponding to $\theta_A(0) = \theta_B(0) = 0.495$. (Note that the A and B distributions are complementary. A narrow lane of empty sites separates between them.) b. The long-time (near steady-state) structure of the overlayer developing from the initial condition in Fig. 5a after 4000 MCS, $\theta_A^* \approx \theta_B^* \approx 0.29$. c. The long-time overlayer pattern developing from an initially empty lattice (i.e., $\theta_A(0) = \theta_B(0) = 0$).

and have not analyzed the adlayer structure. This issue has been addressed by Ziff and Fichthorn,[15] who found that the cluster size distribution can be approximated by the hyperbolic form, $n_s \sim s^{-\tau}$ with $\tau \sim 2.05$. Also, by analyzing the clusters' radii of gyration as a function of their sizes, $R_g \sim s^{1/D}$, they concluded that the aggregates are characterized by a fractal dimension $D = 1.90 \pm 0.03$, similar to that of percolation clusters.[11-13] More recently, Meakin and Scalapino[27] have analyzed the adlayer's temporal evolution using large-scale MC simulations. These authors found that at long times the fraction of vacant sites decreases very slowly according to $\theta_0 = (1 - \theta_A - \theta_B) \sim t^{-w}$ with $w = 0.055$. Furthermore, they raise doubts if, at all, the system is approaching a steady state.

In our opinion, the latter issue is unambiguously resolved if the system approaches the same behavior starting from different initial conditions. In Fig. 5 we show the overlayer patterns characterizing the system at long times, starting from two different initial conditions (under the same impingement flux). In one case, the simulation begins by adding randomly A and B

molecules to an empty surface. In the second, the surface has been precovered by some (arbitrarily chosen) patches of A's and B's with lanes of empty sites separating between them. In the latter case, A and B are randomly added to the vacant sites, and the system develops (much faster than in the first case) by instantaneous annihilation of any A–B pair. The long-time patterns corresponding to the two computer experiments appear very similar. Furthermore, in both cases $\theta_A(=\theta_B)$ approaches the same asymptotic value $\theta_A^* = \theta^* = 0.28 \pm 0.02$, in one case from below $(\theta_A(t=0)=0)$ and in the other from above $(\theta_A(t=0)\sim 0.5)$.

A more quantitative measure of the overlayer structure at steady state is provided by the radial pair correlation functions,

$$g_{ij}(r) = \frac{1}{\theta_i \theta_j} \langle \rho_i(\mathbf{r}')\rho_j(\mathbf{r}'')\rangle, \qquad (5)$$

where $\rho_i(\mathbf{r})$ is the local density of i molecules (i = A, B, j = A, B) at point r, and $r = |\mathbf{r}' - \mathbf{r}''|$. Since the particle positions are restricted to lattice points, we have in our case $\rho_i(\mathbf{r}) = \rho_i(\mathbf{r}_k) = \delta_i(\mathbf{r}_k)$, meaning that $\rho_i(\mathbf{r}_k) = 1$ if an i molecule occupies the lattice site at $\mathbf{r}_k$ and 0 otherwise. The averaging is over all lattice points. Figure 6 displays $g_{AA}(r)$ $(=g_{BB}(r))$ and $g_{AB}(r)$ when the system approaches its steady-state regime. As expected, g_{AA} and g_{AB} reveal complementary behavior. The correlation length characteristic of the A-clusters extends several lattice units, $\xi_{ii} \sim 10$. It should be noted that this result is independent of the initial state of the system.

We are currently analyzing various other structural and temporal characteristics of the overlayer pattern in the A + B → 0 system.[29] We are also examining the role of competing factors such as particle diffusion and adsorbate interactions. In particular, it is clear that fast particle diffusion acts against the organization of A's and B's in separate domains. Furthermore, if the A + B annihilation reaction occurs with high probability, fast diffusion will significantly enhance the rate of reaction, both due to increasing the frequency of A + B collisions and (consequently) by enhancing the fraction of vacant sites onto which gas phase molecules can stick and react. The dependence of the fraction of occupied sites near steady state, $\theta^* = \theta_A^* = \theta_B^*$, as a function of the diffusion rate is shown in Fig. 7. The diffusion rate d is measured here relative to the flux of molecules impinging on the surface from the gas phase. More precisely, $d = w_l/J$ where w_l is the frequency characteristic of a lateral jump of an A or a B molecule into a neighboring vacant site, and J is the number of (either A or B) molecules striking a lattice site per unit time. As expected, θ^* falls off rapidly with d.

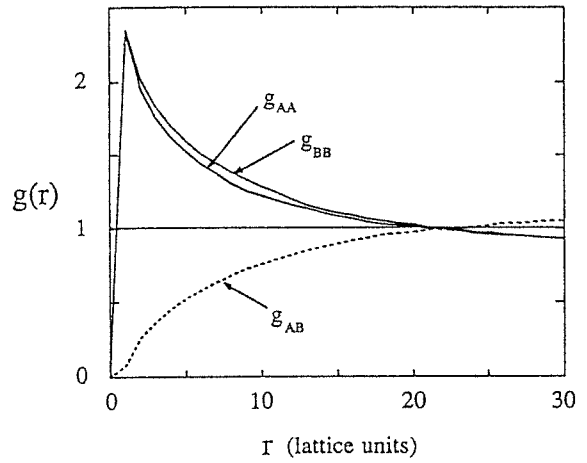

Fig. 6. The radial pair correlation function of the steady-state overlayer generated by the A + B → 0 annihilation reaction, with no particle diffusion. Averaged over five simulations.

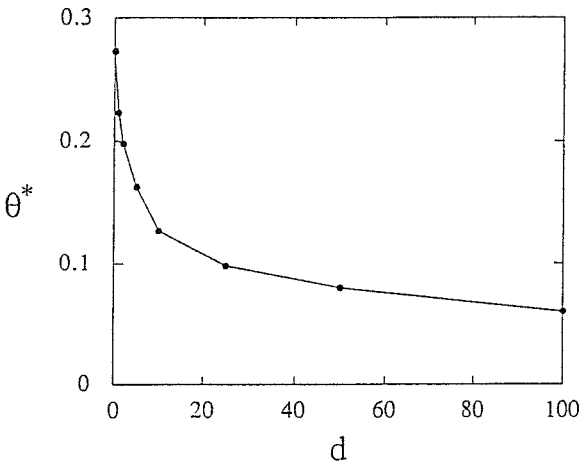

Fig. 7. Near steady-state coverages θ^* $(=\theta_A^* = \theta_B^*)$ after 2000 MCS of the A + B → 0 reactive system as a function of the diffusion rate d (under constant $J_A = J_B$ impingement flux). The dots are the results of simulations on an initially empty 100 × 100 lattice.

Finally, it should be mentioned that various authors have studied the effects of reactive events of the type A + B → 0 or A + A → 0 in systems of rapidly diffusing particles, using diffusion equations and related approaches.[30–36] Although most of these studies focus on different aspects of the problem or are concerned with the transient annihilation reaction alone, some of them are relevant to the problem described in this section and will be discussed elsewhere.[29]

Acknowledgments. We are pleased to dedicate this article to the special issue of the *Israel Journal of Chemistry* in honor of R.D. Levine and J. Jortner, our mentors and colleagues. This research has been partly supported by the V.D.I. Düsseldorf, FRG, through the National Council for Research and Development, Israel and the Fund for Basic Research administered by the Israeli Academy of Sciences. The Fritz Haber Research Center is supported by the Minerva Gesellschaft für die Forschung, mbH, FRG.

REFERENCES

(1) See, e.g., Grest, G.S.; Srolovitz, D.J. *Phys. Rev. B*, 1984, **30**: 5150; Gunton, J.D.; San Miguel, M.; Sahni, P.S. In *Phase Transitions*, Vol. 8, Chapter 3; Domb, C.; Lebowitz, J.L., Eds.; Academic Press: London, 1983; Binder, K. *Physica*, 1986, **140A**: 35; Sadiq, A.; Binder, K. *J. Stat. Phys.*, 1984, **35**: 617; Huse, D.A. *Phys. Rev. B*, 1986, **34**: 7834; Amar, J.G.; Sullivan, F.E.; Mountain, R.D. *Phys. Rev. B*, 1988, **37**: 196; Roland, C.; Grant, M. *Phys. Rev. Lett.*, 1988, **60**: 2657; Gunton, J.D. *J. Vac. Sci. Technol. A*, 1988, **6**: 646.

(2) Silverberg, M.; Ben-Shaul, A.; Rebentrost, F. *J. Chem. Phys.*, 1985, **83**: 6501.

(3) Silverberg, M.; Ben-Shaul, A. *J. Chem. Phys.*, 1987, **87**: 3178; see also *Chem. Phys. Lett.*, 1987, **134**: 491.

(4) Silverberg, M.; Ben-Shaul, A. *Surf. Sci.*, 1989, **214**: 43; see also *J. Stat. Phys.*, 1988, **52**: 1179.

(5) Hood, E.S.; Toby, B.H.; Weinberg, W.H. *Phys. Rev. Lett.*, 1985, **55**: 2437.

(6) (a) Evans, J.W.; Nord, R.S. *J. Vac. Sci. Technol. A*, 1987, **5**: 1040. (b) Evans, J.W.; Nord, R.S.; Rabaey, J.A. *Phys. Rev. B*, 1988, **37**: 8589.

(7) (a) Hill, T.L. *Statistical Mechanics*; McGraw-Hill: New York, 1956. (b) Hill, T.L. *Introduction to Statistical Thermodynamics*; Addison–Wesley: Reading, MA, 1960.

(8) See, e.g., Lagally, M.G.; Wang, G.-C.; Lu, T.-M. *Crit. Rev. Solid State Sci. Mater. Sci.*, 1978, 7: 233; Wang, G.-C.; Lu, T.-M. *Phys. Rev. Lett.*, 1983, **50**: 2014; Williams, E.D.; Weinberg, W.H.; Sobrero, A.C. *J. Chem. Phys.*, 1982, **76**: 1150; Tringides, M.; Wu, P.K.; Moritz, W.; Lagally, M. *Ber. Bunsenges. Phys. Chem.*, 1986, **90**: 277; Poelsma, B.; Verheij, L.K.; Comsa, G. *Phys. Rev. Lett.*, 1983, **51**: 2410.

(9) Stuve, E.M.; Madix, R.J.; Brundle, C. *Surf. Sci.*, 1984, **146**: 155.

(10) (a) Ertl, G. In *Catalysis*, Vol. 4; Anderson, J.R.; Boudart, M., Eds.; Springer-Verlag: Berlin, 1983; p. 210. (b) Engel, T.; Ertl, G. *Adv. Catal.*, 1979, **28**: 1.

(11) Stanley, H.E.; Ostrowsky, N., Eds. *On Growth and Form*; Martinus-Nijhoff Publishers: Dordrecht, 1986.

(12) Jullien, R.; Botet, R. *Aggregation and Fractal Aggregates*; World Scientific Press: Singapore, 1987.

(13) Stauffer, D. *Introduction to Percolation Theory*; Taylor & Francis: London, 1985.

(14) Witten, T.A.; Sanders, L.M. *Phys. Rev. Lett.*, 1981, **47**: 1400.

(15) Ziff, R.M.; Fichthorn, K. *Phys. Rev. B*, 1986, **34**: 2038.

(16) (a) Binder, K., Ed. *Monte Carlo Methods in Statistical Physics*, 2nd Edition; Springer-Verlag: Berlin, 1986. (b) Binder, K., Ed. *Applications of the Monte Carlo Method in Statistical Physics*, 2nd Edition; Springer-Verlag: Berlin, 1987.

(17) Tompkins, F.C. *Chemisorption of Gases on Metals*; Academic Press: London, 1978, and references cited therein.

(18) (a) Kisliuk, P. *J. Phys. Chem. Solids*, 1957, 3: 95. (b) Kisliuk, P. *J. Phys. Chem. Solids*, 1958, **5**: 78.

(19) Becker, O.M.; Ben-Shaul, A. *Phys. Rev. Lett.*, 1988, **61**: 2859.

(20) King, D.A.; Wells, M.G. *Proc. R. Soc. London, Ser. A*, 1974, **339**: 245. See also Weinberg, W.H.; Comrie, C.M.; Lambert, R.M. *J. Catal.*, 1976, **41**: 489.

(21) Becker, O.M.; Ben-Shaul, A.; to be published.

(22) (a) Hinrichsen, E.L.; Feder, J.; Jossang, T. *J. Stat. Phys.*, 1986, **44**: 793, and references cited therein. (b) Nord, R.S.; Evans, J.W. *J. Chem. Phys.*, 1985, **82**: 2795. (c) Schaff, P.; Talbot, J.; Rabeony, H.M.; Reiss, H. *J. Phys. Chem.*, 1988, **92**: 4826. (d) Schaff, P.; Talbot, J. *Phys. Rev. Lett.*, 1989, **62**: 175.

(23) Sanders, D.E.; Evans, J.W. *Phys. Rev. A*, 1988, **38**: 4186.

(24) Anderson, S.R.; Family, F. *Phys. Rev. A*, 1988, **38**: 4198.

(25) Ziff, R.M.; Gulari, E.; Barshad, Y. *Phys. Rev. Lett.*, 1986, **56**: 2553.

(26) Dickman, R. *Phys. Rev. A*, 1986, **34**: 4246.

(27) Meakin, P.; Scalapino, D.J. *J. Chem. Phys.*, 1987, **87**: 731.

(28) Wicke, E.; Kumman, P.; Keil, W.; Schiefler, J. *Ber. Bunsenges. Phys. Chem.*, 1980, **84**: 315.

(29) Becker, O.M.; Ben-Shaul, A.; to be published.

(30) Ovchinnikov, A.A.; Zeldovich, Ya.B. *Chem. Phys.*, 1978, **28**: 215.

(31) Toussaint, D.; Wilczek, F. *J. Chem. Phys.*, 1983, **78**: 2642.

(32) (a) Anacker, L.W.; Kopelman, R. *Phys. Rev. Lett.*, 1987, **58**: 289; *J. Phys. Chem.*, 1987, **91**: 5555. (b) Lindenberg, K.; West, B.J.; Kopelman, R. *Phys. Rev. Lett.*, 1988, **60**: 1777. (c) Anacker, L.W.; Parson, R.P.; Kopelman, R. *J. Phys. Chem.*, 1985, **89**: 4758.

(33) Kanno, S. *Prog. Theor. Phys.*, 1988, **79**: 721.

(34) Meakin, P.; Stanley, H.E. *J. Phys. A*, 1984, **17**: L173.

(35) Kang, K.; Render, S. *Phys. Rev. Lett.*, 1984, **52**: 955.

(36) Yi-Cheng, Z. *Phys. Rev. Lett.*, 1987, **59**: 1726.